PHASE MAPPING OF IRON-BASED RAPIDLY QUENCHED ALLOYS USING PRECESSION ELECTRON DIFFRACTION

P. Švec, I. Janotová, J. Hoško, D. M. Kepaptsoglou[1], I. Maťko, D. Janičkovič, P. Švec Sr.

Institute of Physics, Slovak Academy of Sciences, Bratislava, Slovak Republic
[1]SuperSTEM Laboratory, STFC Daresbury, United Kingdom
E-mail: fyzisvec@savba.sk

Received 15 May 2013; accepted 21 May 2013

1. Introduction

Amorphous alloy systems, usually prepared by rapid quenching of the melt, are as a rule thermally processed to maximize their physical properties, e. g. magnetic, or mechanical. Thermal treatment may either leave the structure in original amorphous state or transform it into a composite consisting of small crystalline grains with sizes ranging from a few to hundreds of nanometers embedded in remaining amorphous matrix. Determination of phases and orientation of the nanograins is, alongside with phase content quantification and size distribution, of major importance.

While in classical solids with grain sizes of micron or even submicron sizes this problem is solved by using electron backscattered diffraction (EBSD) in scanning electron microscopes (SEM), this method can be applied only with difficulties to smaller grains. Transmission electron microscopy (TEM), due to its high spatial resolution, is very convenient for imaging and analysis of nanocrystals. By forming a parallel beam in TEM and selecting a crystal with an aperture, or by forming a fine convergent beam of only a few nanometres diameter, electron diffraction (ED) pattern can be recorded from crystals too small to be studied by either EBSD or X-ray diffraction. The study of crystals at nanoscale or even atomic level by electrons – electron crystallography – is an important complement to X-ray crystallography. Among the main advantages of structure determinations by electron crystallography compared to X-ray diffraction are the facts that crystals several orders of magnitude smaller than those needed for X-ray diffraction can be studied and the phases of the crystallographic structure factors, which are lost in X-ray diffraction, are present in TEM images. Small electron beam spot sizes allow structure studies of individual nanograins by electron diffraction.

Recently developed experimental technique reducing dynamical effects in electron diffraction data and thus allowing the use of ED pattern intensities directly for ab-initio structure determination is precession electron diffraction (PED) [1, 2, 3]. In this technique, the incident beam is precessed in a hollow cone around the central zone axis direction as the data are collected. The collected diffraction data show reduced dynamical effects because there are far fewer simultaneously excited reflections in the off-zone condition. In addition, the precession integrates the diffraction intensities through the Bragg condition, which provides data sets significantly less affected by minor sample tilts and makes interpretations of pattern symmetry more reliable. This technique is equivalent to the Buerger precession technique [4], used in X-ray diffraction where the specimen is precessed with respect to the X-ray incident beam. In the electron precession technique, it is the electron beam, which is tilted and precessed along a cone surface having a common axis with the TEM optical axis and with the zone axis. As a result of this precession movement only a very few reflections are simultaneously excited, much more reflections are visible in ED pattern, the diffracted

intensity of the beams is the integrated intensity and the resulting diffraction pattern can be considered less dynamical. By precessing an incident beam at a constant angle close to zone axis condition in combination with a similar counter-precession (descan) of the ED pattern below the specimen, quasi-kinematic electron diffraction patterns are obtained. Simultaneous scanning of the focused electron beam over a selected area of the investigated sample in steps as small as few nanometers and beam precession allows structure mapping of individual grains. This can be achieved using a TEM accessory DigiStar [5]; its working principle is shown in Fig. 1.

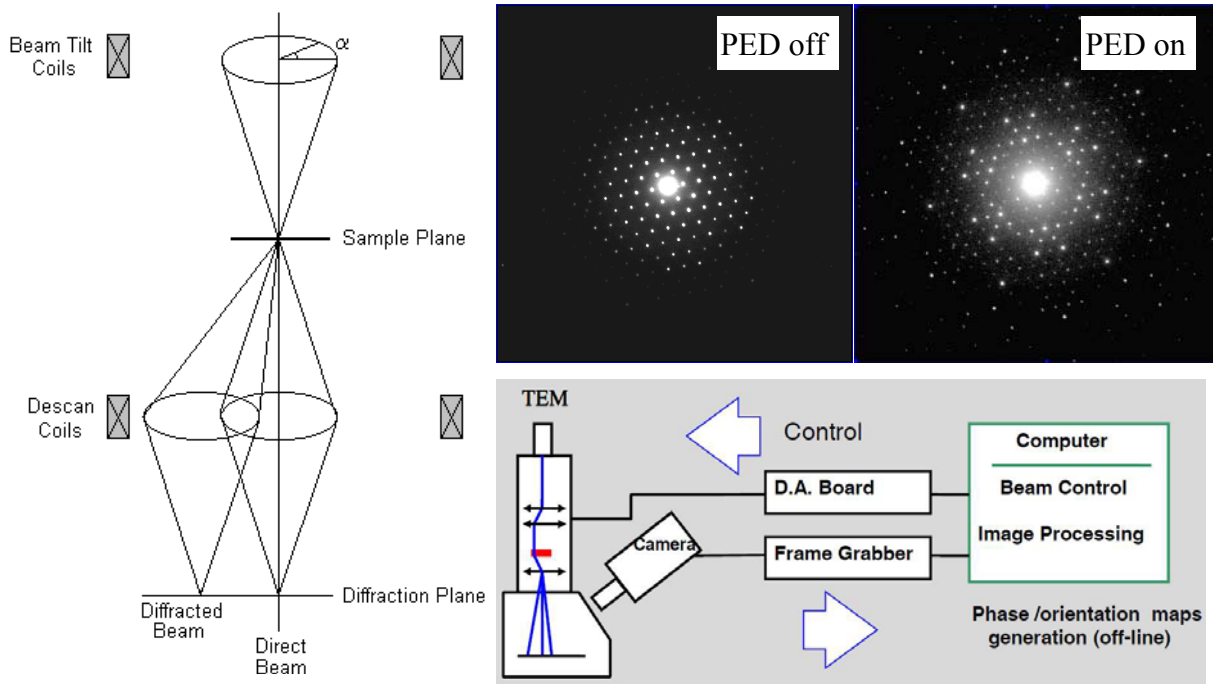

Fig.1: *Application of precession and counter-precession (descan) to the beam movement in TEM and ED patterns [2] of a Garnet monocrystal in (111) orientation without and with beam precession (PED) showing the reduction of dynamical contribution to all reflections. Bottom right – block scheme of precession electron diffraction device DigiStar [5].*

The present contribution is focused on application of PED and phase/orientation mapping of nanocrystals of bcc-Fe formed during the first crystallization stage of amorphous Fe-Co-Si-B ribbon, which has been described previously [6].

2. Experimental

Master alloy of composition $Fe_{60}Co_{20}Si_5B_{15}$ was prepared from elements with purity better than 99.5%. Amorphous ribbons 10mm wide and approximately 25 microns thick were prepared by planar flow casting. The composition and as-cast amorphous state of the ribbons were verified by inductively coupled plasma spectroscopy and X-ray diffraction, respectively. Phase transformations as a function of temperature and time were monitored by high-precision four-probe electrical resistivity measurements with accuracy better than 0.01%. in a vacuum furnace. X-ray diffraction measurements were performed using Cu Kα radiation with a graphite monochromator in the diffracted beam. Transmission electron microscopy (TEM), selected area electron diffraction (SAED) and PED were performed on annealed samples prepared by ion-beam polishing in TEM JEOL 2000FX equipped with DigiStar.

3. Crystallization stages

The evolution of electrical resistivity under linear heating and isothermal regimes is shown in Fig. 2, where two distinct transformation stages (resistivity decrease) can be observed. The structures formed in each stage and described in [6] are shown in Fig. 3.

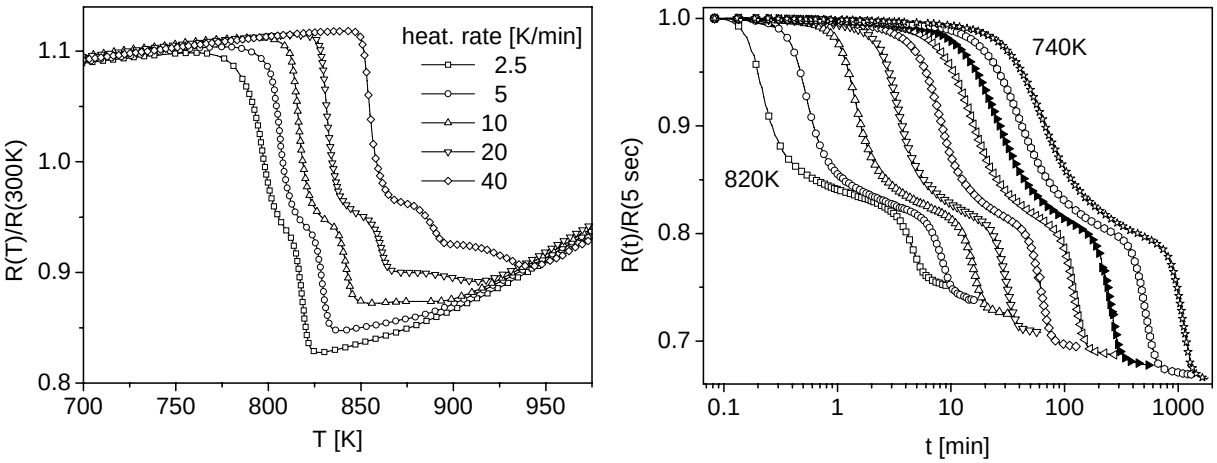

Fig.2: *Temperature and time dependencies of electrical resistivityR(T, t) in the course of two-stage crystallization of amorphous Fe-Co-Si-B. Bold symbols on the curve in the left image indicate isothermal annealing temperature 760 K used in further study.*

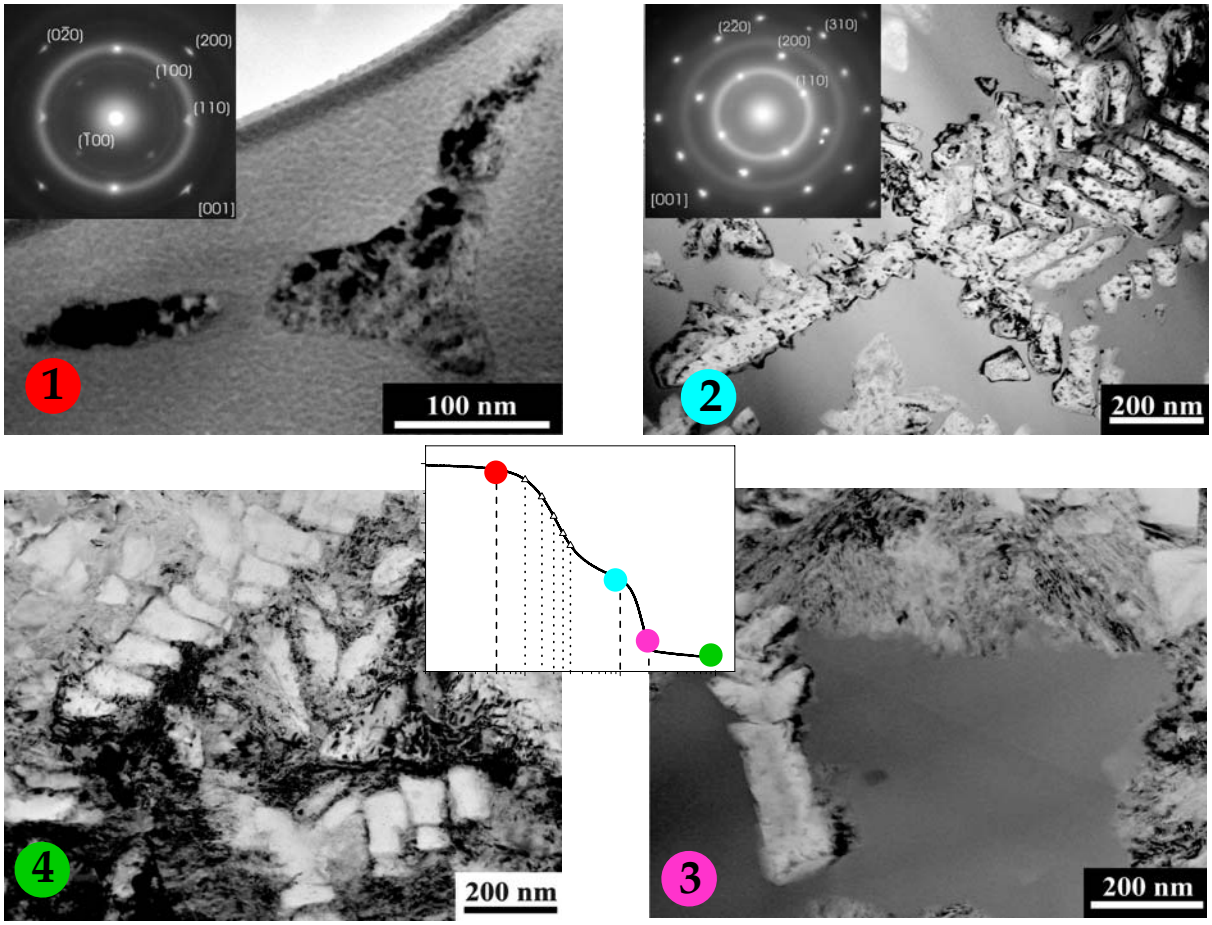

Fig.3: *Microstructures formed after annealing at 760 K for 3, 100, 200 and 1000 min, respectively, denoted by consecutive numbers. Insets in images 1 and 2 show SAED patterns of the forming bcc-Fe phase. Inset in the middle is the R(t) isotherm at 760 K [6].*

4. Precession electron diffraction and phase mapping

Sample annealed at 760 K for 100 min, where the formation of bcc-Fe from amorphous matrix, as witnessed by the ED inset in image 2 of Fig. 3, is almost completed, has been selected for PED and phase/orientation mapping. The effect of precession on the SAED pattern is shown in Fig. 4. The SAED pattern was taken from the central part of the image, where both the amorphous matrix (diffuse halo) and the newly formed bcc-Fe with lattice parameter a-0.254 nm [6] evidenced by sharp diffraction spots are present. DP taken without precession shows a certain amount of dynamic scattering affecting the intensities of the individual diffraction spots. Precession of diffracting beam of 0.6 angular degrees markedly reduces dynamical variations of the spot intensities. Furthermore, the DP is more complete even without any additional sample orientation into the zone axis – note that there are 7 and 5 identifiable diffraction spots in the top and bottom rows, respectively, compared to 3 and 3 spots in the ED pattern taken without precession.

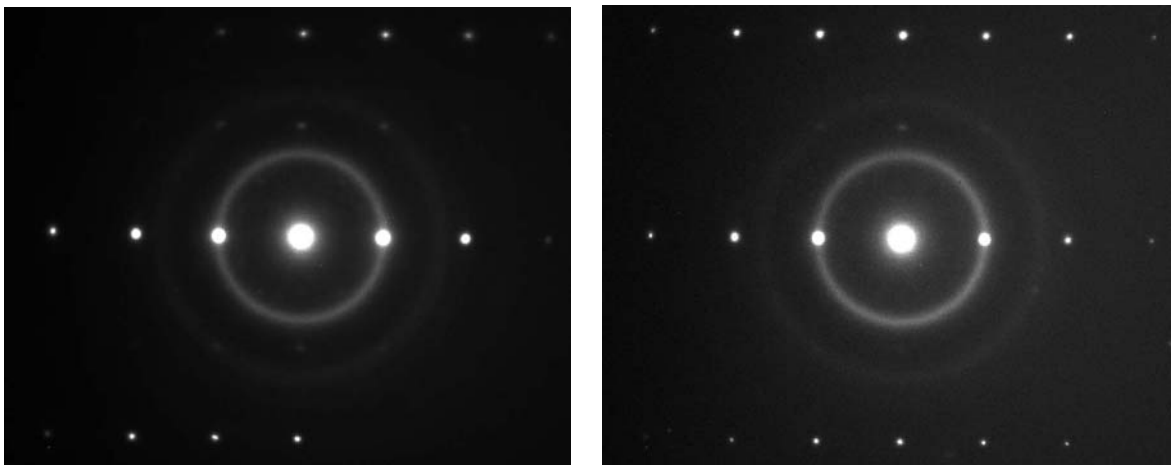

Fig.4: *SAED patterns from the central area of image 2 in Fig. 3 without precession of the incident beam (left) and with precession of 0.6 angular degrees (right).*

Phase/orientation mapping was performed on the same sample, however, at different area due to contamination of the sample by electron beam. Dimensions of the mapped area were 640 x 640 nm with 80 sampling points in horizontal and vertical directions (sampling step 8 nm). In all points diffraction patterns were recorded, creating a bank of 6400 images with resolution of 144 x 144 pixels, sufficient for post-acquisition processing. Indexing and refining of the image bank was performed against the a-priori the known two-phase content of the area, namely bcc-Fe (space group Im-3m with lattice parameter a = 0.2866nm) and amorphous phase (approximated by structure with space group Fm-3m with large lattice parameter, a = 1.2 nm). The results of the procedure are shown in Fig. 5.

Fig. 5a shows virtual bright field image reconstructed from the intensities of the primary electron beam. In a similar manner, however using selected diffracted spots, virtual dark field images can be reconstructed, as shown in Figs. 5b and c, the latter from the upper intense diffracted spot in the diffraction pattern from Fig. 5d.

Final evaluation of the obtained phase and orientation mapping is shown in Figs. 5e and f, respectively. It can be seen that the complex dendritic-like crystalline structure is reliably indexed as bcc-Fe (red) surrounded by the amorphous featureless matrix (green). Only two major orientations, namely [100] and [111] (compare the colors with the orientation color map shown in Fig. 5h) with only minimal degree of disorientation were observed; black color was assigned to amorphous phase for convenience. The overlay of phase and virtual bright field images (Fig. 5g) shows excellent correlation between the morphology and phase/orientation distribution.

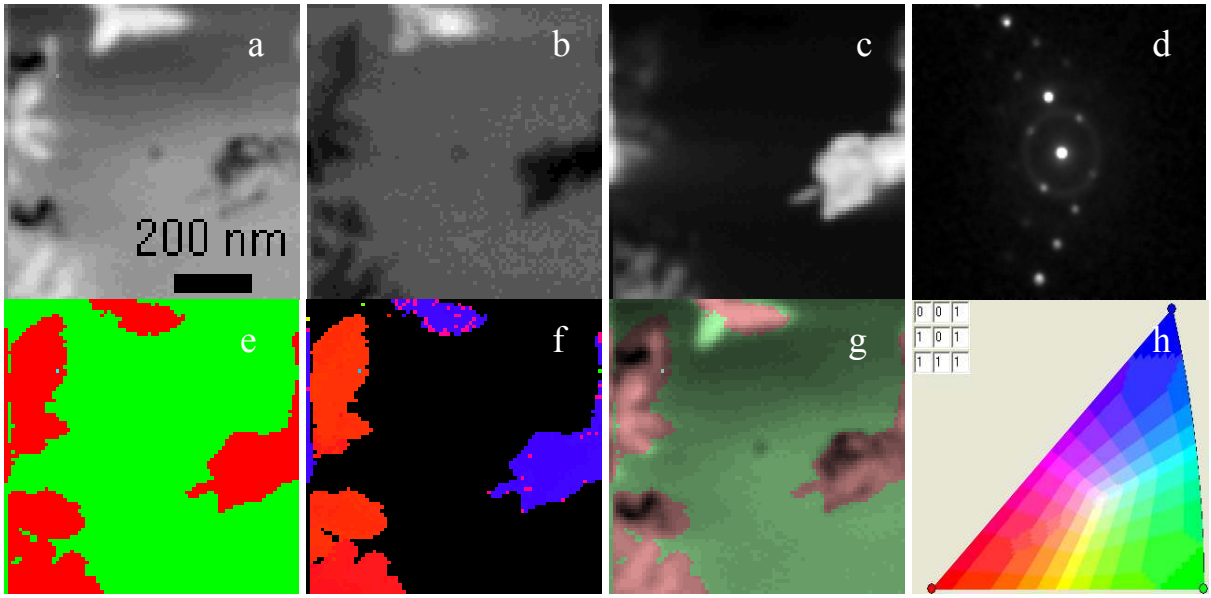

Fig.5: *Results of phase and orientation mapping of 640 x 640 nm area of sample shown in image 2 of Fig. 3. Virtual bright field image (a) of the analyzed area, virtual dark field images (b), (c) from the diffracted spots in ED pattern (d), phase (e) and orientation (f) maps and combined image (g) from phase and virtual bright field image; (h) orientation color map.*

5. Discussion

Detailed inspection of Fig. 3, especially of images 1 and 2, shows that the bcc-Fe phase forming from amorphous matrix, while apparently dendritic-like, is composed of several smaller individual particles. It is of primary interest for understanding the structure of amorphous phase to show whether the mechanism of crystallization is controlled by long-range diffusion of constituent atoms or whether a mechanism different from classical single-atom diffusion is active in controlling the transformation from amorphous systems. Information about orientation of individual particles is very helpful, especially in view of the facts that majority of particles forming apparent "branches" of the pseudo-dendrites are of similar orientation and that the orientations are confined to the three major orientation directions (compare zone axes in insets of images 1 and 2 in Fig. 3 and the orientation map in Fig. 5f) of the cubic Fe-phase with respect to the surface of the ribbon sample. It is also to be noted that SAED inset in image 1 of Fig. 3, corresponding to the early stages of formation of bcc-Fe shows the presence of forbidden reflections (100) due to supersaturation of the Fe-phase with Si (and possibly also with B); this effect is impossible to monitor via X-ray diffraction while due to different electron scattering factors of Fe, Si and B it is visible using electron crystallography. This effect persists during the entire first crystallization stage, suggesting that local structure of the amorphous matrix and of the forming crystalline phase remains chemically unchanged; this observation is corroborated by high-resolution elemental mapping where no significant concentration gradient has been detected at the interface between the amorphous matrix and the crystallizing phase as wel as by thermodynamic considerations [7].

Determination of phase/orientation maps using the DigiStar PED and mapping attachment has significant advantages against using EBSD techniques. While providing similar information set, spatial resolution in TEM is by orders of magnitude higher, sample preparation, compared to complicated and critical preparation of surfaces for EBSD analysis, is identical to that for TEM observations. Time required for PED and TEM mapping is of the order of minutes (against typical hours of EBSD mapping), reducing effects of sample drifts

and other instrumental instabilities leading to decreased resolution. In addition, obtaining quasi-kinematic ED patterns reduces uncertainty in phase and orientation mapping alongside with the possibility of ab-initio structure calculations. Important asset of PED lies also in decreased requirements on exact phase zone orientation with respect to the primary beam, reducing need for sample tilting and in increasing productivity of the ED analysis

6. Conclusions

Using precession electron diffraction and phase/orientation mapping the formation of primary crystalline phase, bcc-Fe, from amorphous Fe-Co-Si-B has been analyzed. Important information about mutual orientation of the phase in individual submicron grains as well as against the sample surface has been obtained. This information contributes to the understanding of micromechanisms controlling crystallization from amorphous rapidly quenched structure and of the structure of the original amorphous state.

The presented technique due to its high spatial resolution, speed and information content provided complements well classical techniques, especially in nanocrystalline materials.

Acknowledgement

This work was supported by the ASFEU project Competence Center for New Materials, Advanced Technologies and Energy, Activity 2.3, ITMS code 26240220073, supported by the Research and Development Operational Program funded by the ERDF (90%). Support of the projects APVV-SK-PL-0043-12, VEGA 2/0111/11 and CEX FUN-MAT is also gratefully acknowledged.

References:

[1] R Vincent, P. A Midgley, Ultramicroscopy **53**, 271 (1994).
[2] C. S. Own, A. K Subramanian, L. D. Marks, Microscopy and Microanalysis **10**, 96 (2004).
[3] J.Gjonnes, V.Hansen, A. Krerneland Microscopy and Microanalysis **10**, 16 (2004).
[4] J.-L. Staudenmann, R. D. Horning, R. D. Knox, J. Appl. Cryst. **20**, 210 (1987).
[5] E. F. Rauch, J. Portillo, S. Nicolopoulos, D. Bultreys, S. Rouvimov, P. Moeck, Z. Kristallogr. **225**, 103 (2010).
[6] D. M. Kepaptsoglou, P. Svec, D. Janickovic, E. Hristoforou, Journal of Alloys and Compounds **434–435**, 211 (2007).
[7] K. Kristiakova, P. Svec: Phys. Rev. B **64,** 014204 (2001).